NUMERICAL COMPARISON OF SAVONIUS TURBINE AS A ROTOR FOR GRAVITATIONAL VORTEX TURBINE WITH STANDARD ROTOR

Alejandro Ruiz Sánchez[1]*, Jorge Andrés Sierra Del Rio[1,2]*, Edwin Correa Quintana[1], Daniel Sanín-Villa[2]

[1] Deparment of Mechatronics Engineering, MATyER, Instituto Tecnológico Metropolitano, 050034, Medellín, Colombia
[2] Deparment of Mechanical, GIAM, Institución Universitaria Pascual Bravo, 050054, Medellín, Colombia

*alejandroruiz9433@correo.itm.edu.co

The generated kinetic energy of a water vortex can be transformed into electrical energy by a Gravitational Water Vortex Power Plant. Which is a new and green alternative for a conventional power plant that can induce/create a vortex without great civil construction. Previous studies focus their objective on tank design and vortex formation inside it (to study the fluid outlet velocity). However, the rotor design is a parameter that affects directly in turbine performance. The main purpose of this study is to compare numerically with the Ansys software the Savonius turbine as a Gravitational Vortex turbine rotor with the standard rotor (straight blades). The study showed that the straight-bladed rotor performed better with a generated torque of approximately 1.1 Nm, compared to 0.6 Nm generated by the Savonius. In conclusion, it was shown that the design of the rotor for the gravitational vortex turbine considerably affects its performance, where it can be increased or decreased by up to 30% difference.

Keywords: vortex, rotor, savonius, torque, cfd

1 INTRODUCTION

The gravitational vortex turbine (GVT) is an alternative to renewable energies. It is a small-scale turbine which transforms the kinetic energy of the fluid by the formation of a vortex into electrical energy through a generator [1]. Figure 1 exemplifies the operation and parts of the turbine (designated as standard tank). The geometry is configured, in the direction of flow through an open channel of rectangular section, which leads and stabilizes the flow of water that has been derived from the river. Then through an eccentric reduction while maintaining the height of the channel, the flow is accelerated. The Fluid just before entering the upper part of the chamber tank, which is generally configured as a cylindrical tank with a circular and concentric outlet located at the bottom respect to the level of the inlet channel. The fluid enters horizontally and tangentially, but due to the circular geometry of the tank and the difference in level between the entrance and outlet hole of the chamber, a rotation of the fluid is induced with respect to the exit orifice known as a gravitational vortex, which is form due to the joint action of the gravitational force and the Coriolis force [2]. For a streamline, the path that the water takes inside the chamber tank can be represented by a spiral that rotates around the axis of the air core, which is formed by conservation of momentum between two fluids: water and air in this case.

To characterize the vortex induced by the cylindrical tank, cylindrical velocity coordinates are established, characterized by tangential velocity, radial velocity, and axial velocity component. For a streamline that enters the cylindrical tank from the inlet channel, initially the tangential velocity component predominates over the dynamics of the flow, which increases as it approaches the center of rotation of the fluid, guaranteeing the conservation of mass inside the chamber. This increase in tangential velocity represents an opportunity for the transfer of rotational kinetic energy towards the rotor shaft, which is made up of a number and geometry of blades defined according to the conditions of the velocity field present inside the turbine chamber. An appropriate geometry of the blade allows the rotor to extract as much energy from the fluid as possible, to then convert it into electrical energy by means of a generator. Once the fluid passes through the rotor, it continues the spiral path towards the outlet, this due to the action of gravity, causing the axial component of the velocity to increase as the streamline approaches the outlet.

The main objective of this study is to compare numerically the torque generated by a Savonius turbine as a rotor for the GVT with a standard rotor (straight blades) using the Ansys commercial software.
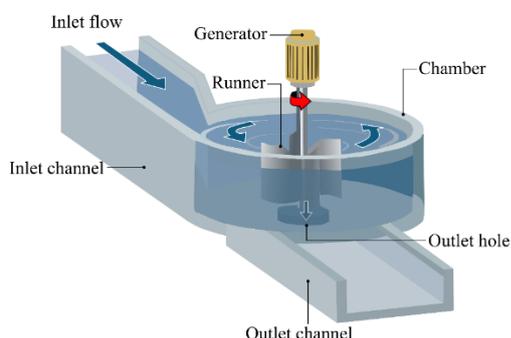

Figure 1. Gravitational Vortex Turbine parts.

2 PREVIOUS STUDIES

2.1 Studies

The studies that have been carried out around the GVT have focused mainly on the tank design and the measurement variable is the outlet velocity of the fluid in the turbine outlet hole. Table 1 summarizes the main results found in the literature. It should be noted that no optimal geometry is reported in numerical and experimental studies. Some parameters for the design of the turbine tank are recommended, but the ideal design or type of rotor for the turbine is not mentioned. On the other hand, the methodology proposed by the authors in the numerical studies is not clear. Where the efficiency of the turbine cannot be determined [3]. However, it is not easy to calculate the efficiency of this turbine. Because due its several geometry parameters, like tank design, inlet channel measures and rotor design have a high influence in the GVT performance.

Nowadays, the most article developed are numerically in the commercial software Ansys. Those studies can determinate the optimal geometry parameters combination to give the highest performance for the turbine.

Table 1. GVT studies.

Parameter	Study	Main result	Reference
Inlet channel height	CFD and experimental	Difference between 0% and 7%	[4], [5] [6]
Numerical and theoretical comparison	CFD and theoretical	Difference upper 20%	[7]
Turbulence model	Analytic, CFD and experimental	BSL RMS	[8]
Tank geometry	CFD and experimental	Conical	[9]
		Cylindrical	[10]
		Conical and Convex	[11]
Tank diameter	CFD	0.8m	[12], [13]
Notch angle		70°	
Inlet channel width		0.125D	
Angle cone		23°	
Tank height		0.2D	
Outlet hole diameter for conical tank		0.3D	
Outlet and tank diameter ratio (d/D)		2.5	
Outlet hole diameter	CFD and experimental	0.14D – 0.18D	[14], [15]
Economic evaluation	Experimental	Economic feasibility	[16]

2.2 GVT installed

Table 2 shows the GVTs installed that have been found to date worldwide. It is observed that Europe is the continent with the most installed (9), followed by Asia (3), South America (2) and Oceania (1). It should be emphasized that the power generated by each turbine depends on its use (domestic or machinery). For this reason, the Swiss turbine stands out for being the largest power generator at a lower flow rate and height. It is also worth noting that between Italy, Austria, and Germany they have seven (7) installed turbines, demonstrating the superiority in GVT installed. To exemplify Table 2, the calculation of the electrical power of (1) [1] was taken.

$$P_{eléctrica} = Q.\rho.h.g.n_t \tag{1}$$

Where Q if fluid flow, ρ is fluid density, h is fluid height, g is gravitational force and n_t is the efficiency of the TVG (where the generator has an efficiency of 90%). However, the calculation of turbine efficiency is not concise in the literature, and in some cases, it is not mentioned [17].

Table 2. GVT installed worldwide

Country	City	Year	Height (m)	Flow (m³/s)	Power (kW)
Swiss [18]	Schöftland	2009	1.5	1	15
Indonesia [19]	Bali	2015	1.8	1	15
Chile [20]	Doñihue	2017	2.1	2	15
Australia [21]	Marysville	2013	0.6	0.1	11

Journal of Applied Engineering Science

Vol. 21, No. 1, 2023
www.engineeringscience.rs

publishing

Alejandro Ruiz Sánchez et al. - Numerical comparison of savonius turbine as a rotor for gravitational vortex turbine with standard rotor

Country	City	Year	Height (m)	Flow (m³/s)	Power (kW)
Italy [22]	Sureste Sesto Campano	2017	1.5	1	9
Italy [22]	Noreste Bivio Mortola	2017	1.8	0.8	9
Thailand [22]	Oeste Taksinmaharat	2014	1.5	1	8.5
Austria [1]	Obergrafendorf	2005	0.9	0.9	8.3
Peru [22]	Junin	2016	1.4	0.9	7.2
Germany [22]	Wesentz, Sachsen	2013	1.2	0.5	6
Germany [22]	Niedersfel, Winterberg	2012	1.4	0.5	4.7
Lithuania [22]	Este Kaunas	2010	1.5	0.5	4.4
Italy [22]	Suroeste San Vito	2014	0.4	0.9	4
Austria [22]	Norte St. Veit an der Glan	2011	0.9	0.7	3.3
Nepal [23]	Katmandú	2016	1.5	0.2	1.6

3 METHODOLOGY

3.1 Governing Equations

Both fluids (air and water) are sharing the same velocity fields and turbulence. The governing equations for the unsteady, viscous and vortex formation turbulent flow are continuity and Navier Stokes described [24] in Eq. (2) and Eq. (3) respectively:

$$\frac{\partial v_r}{\partial r} + \frac{\partial v_z}{\partial Z} + \frac{v_r}{r} = 0 \qquad (1)$$

$$\frac{\partial \bar{u}}{\partial t} + \bar{u} \cdot (\nabla \bar{u}) = \frac{-1}{\rho}\nabla p + v\nabla^2\bar{u} + \bar{g} \qquad (2)$$

Where g, v and ρ are gravitational acceleration, viscosity, and density respectively. $\bar{u}$ represents velocity vector and it is defined in Eq (4) and ∇ reduces the partial derivation in each component (x, y, z) and it is explained by Eq (5).

$$\bar{u} = (u, y, w) \qquad (3)$$

$$\nabla = \frac{\partial}{\partial x}, \frac{\partial}{\partial y}, \frac{\partial}{\partial z} \qquad (4)$$

3.2 Geometry

Figure 2 represents the GVT dimensions. This was divided into two main parts to better exemplify the turbine. Figure 2.a represents the inlet channel width (wc) and length of inlet channel (lc) and area reduction (lra), the area reduction angle (α), the tank diameter (D), cone (DC) and outlet hole (d). Figure 2.b exemplifies the other part of the turbine, in which you can see the height of the channel (HC) and the cone for the outlet hole (hc).
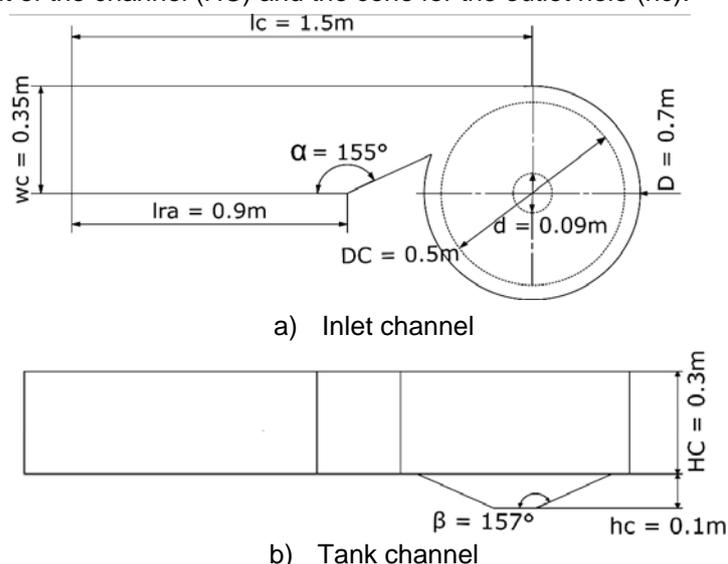

a)   Inlet channel

b)   Tank channel

Figure 2. GVT dimensions

Journal of Applied Engineering Science

Vol. 21, No. 1, 2023
www.engineeringscience.rs

iipp
publishing

Alejandro Ruiz Sánchez et al. - Numerical comparison of savonius turbine as a rotor for gravitational vortex turbine with standard rotor

Figure 3.a represents the Savonius rotor that will be used in this study. This rotor has a height of 0.13m, a diameter of 0.2m, a blade thickness of 3mm and two blades as suggested by [25]. Worth noting, the blades numbers of present rotor were selected according of turbine performance in its normal functioning as a water turbine. The authors want to compare the Savonius rotor with its geometry that guarantees its best performance as a water turbine with a standard rotor. Savonius rotor will be compared with the standard rotor with straight blades, it has the same dimensions (0.13m of diameter, 0.2m of height and 3mm of blade thickness) with the variation that 4 straight blades are configured. Figure 3.b represents the standard rotor.

a)   Savonius rotor

b)   Standard rotor

Figure 3. Savonius rotor

A simulation of GVT without rotor was carried out to stablish the rotor position and diameter. The same dimensions described in Figure 2 were selected and the same boundary conditions configured described in next section (*Discretization Process and Boundary Conditions*) were implemented. Figure 4 shows a water volume fraction contour of this simulation. In this figure it can be seen the symmetric vortex formed into GVT tank. The rotor diameter (dr) and rotor height (hr) were selected according to interface between water (red) and air (blue). The beginning to choose the *dr* was to find an interaction of rotor with higher water fraction than air (> 0.6) but it could not be too higher because, the rotor could destroy the water vortex and the turbine performance goes down.
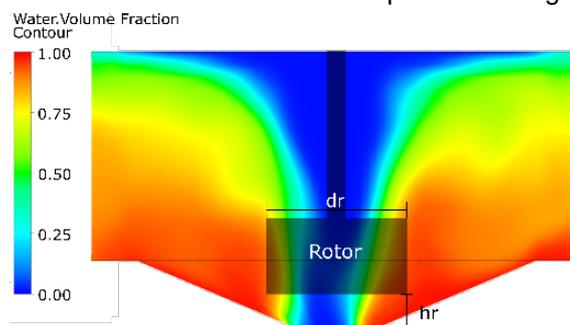

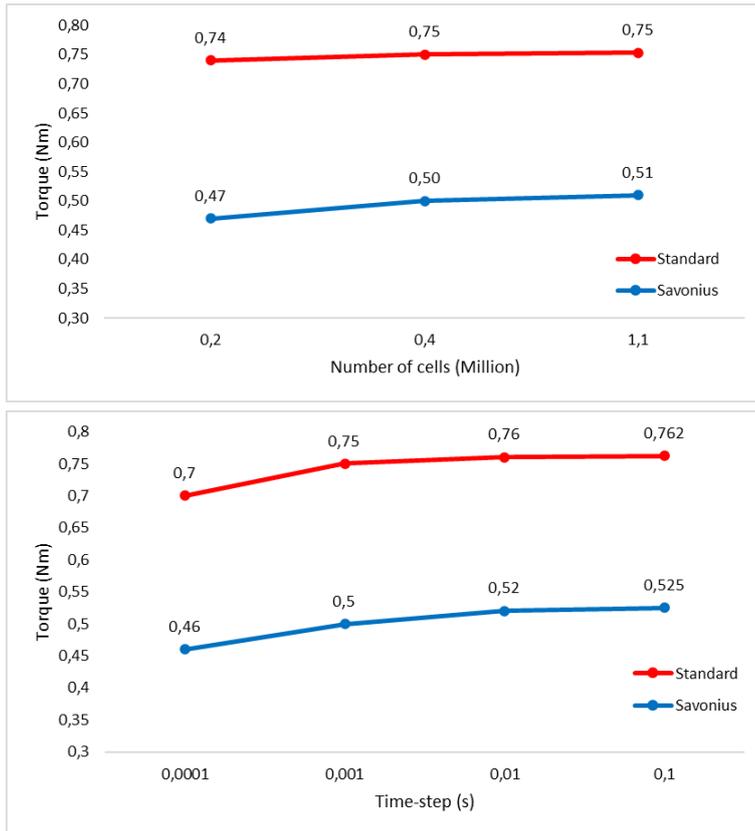Figure 4. Water volume fraction of GVT without rotor

3.3   Discretization Process and Boundary Conditions

Once the rotary and stationary domain was assembled the boundary conditions was configured. The most important feature to consider of this model is the interface between the stationary and rotating model which was "Transient rotor Stator", this was selected because it allows visualizing the movement of the rotor over time (transient simulation) and its interaction with the fluid.

After configuring the boundary conditions for the mesh, the mesh independence study corresponding to the chamber-rotor configuration was performed. The variable monitored in this case was the torque in the Y axis of the rotor (which was used as the vertical axis for this study) at an angular velocity of 10 rpm and expecting to have a difference of less than 5% [26], [27].

Figure 5.a represents the mesh independence for both configurations: Savonius and standard rotor. Simulations were run approximately up to 1.1E6 elements for both rotors where the results do not vary significantly with respect to elements. Therefore, meshes of approximately 4E5 elements for the Savonious rotor and 3.9E5 for the standard rotor were selected to follow the simulations. The meshes were developed in ICEM module, guaranteeing higher quality in elements [28] such quality orthogonal (0.73), aspect ratio (9) and 3x3 determinant (0.84). Addition to metrics described, all elements in meshes were hexahedral elements, this guarantees a lower compute time [29].

In addition to the mesh independence study, a time-step independence study (Δt) was performed for each configuration. Figure 5.b shows the behavior for the two rotors as Δt was changed. The variation between the results was less than 5%, therefore, the Δt of 1ms was established, thus guaranteeing the Courant number less than 1.

Journal of Applied Engineering Science

Vol. 21, No. 1, 2023

www.engineeringscience.rs

iipp
publishing

Alejandro Ruiz Sánchez et al. - Numerical comparison of savonius turbine as a rotor for gravitational vortex turbine with standard rotor

a) Mesh independence

b) Time-step sensibility

Figure 5. Mesh and Time-step independence study

Water and air at 25 °C were selected as fluids, a surface tension coefficient of 0.072 Nm-1 and the selected turbulence model was Baseline Reynold Stress Model (BSL RSM). This turbulence model is a robust model that has a great accuracy to rotational fluids [30] as vortex behavior. The total simulation time was 20 s.

Inlet water velocity was 0.2 m/s. The initial fractions of water and air for GVT was 1 for air and 0 for water. However, the fraction for inlet was 0.99 for water and 0.01 for air. Due inlet channel length, the fluid is stablished before entries the tank. The upper section of GVT was set up as "opening" with a opening pressure o 0 Pa. The walls were configured with no slip condition and the outlet hole was configured as a outlet with a relative pressure of 0 Pa.

4 RESULTS AND DISCUSSION

Once the configuration (boundary and mesh conditions) was established, the simulation was performed varying the angular velocity from 10 rpm to 100 rpm. Figure 6 shows the behavior of the fluid in the GVT chamber. In this, the inlet channel is long enough to stabilize the fluid along it. In this way, the fluid reaches the area reduction completely stable to increase its speed before entering the tank and interacting with the rotor.
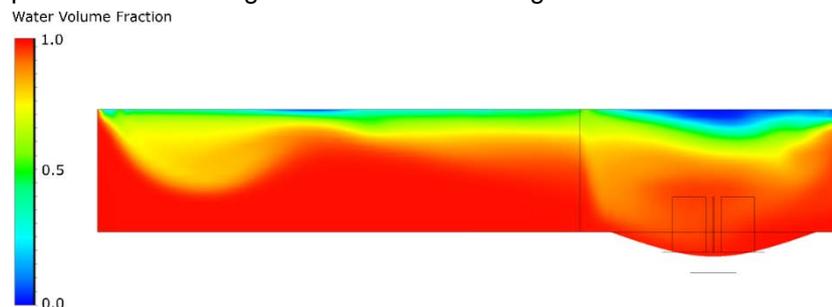

Figure 6. Water volume fraction inside GVT

Figure 7 represents Savonius and standard rotor behavior as the rpm was changed. This graph shows a great difference between both rotors (greater than 30%) at all angular velocities, with the standard rotor being the one with the highest generated torque. On the other hand, both rotors presented the maximum torque at 10 rpm where the standard rotor generated 0.76 Nm and the Savonius rotor 0.50 Nm and the lowest torque generated was presented at 100 rpm with 0.61 and 0.41 Nm for the standard rotor and Savonius respectively. This is to be expected, because the pressure increases the boundary layer effect on the rotor blades on which the fluid impacts, and therefore increases the torque generated.

Journal of Applied Engineering Science

Vol. 21, No. 1, 2023
www.engineeringscience.rs

iipp
publishing

Alejandro Ruiz Sánchez et al. - Numerical comparison of savonius turbine as a rotor for gravitational vortex turbine with standard rotor
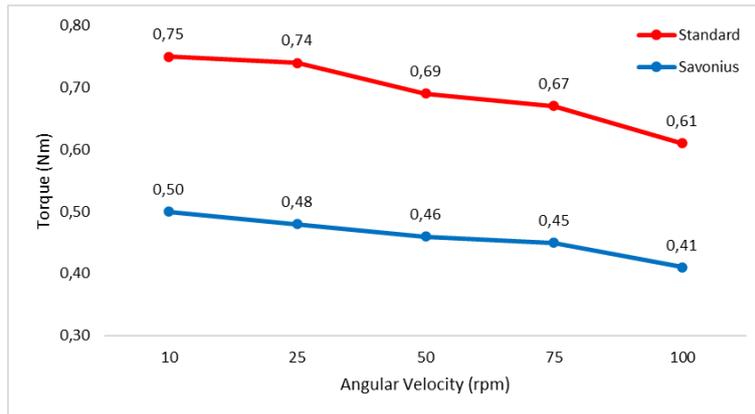
Figure 7. Savonius and standard rotor with different angular velocity

Figure 8 represents the top and isometric view of the fluid streamlines inside the GVT with the two rotors. Figure 8.a represents the standard rotor and Figure 8.b the Savonius rotor. This figure shows how the fluid behaves throughout the GVT path. The size of the particles in streamlines is directly proportional to the fluid velocity. In this way it is verified that the fluid increases its velocity as it approaches and descends through the vortex (tank center). This figure also shows how the fluid behaves with the rotors, which distort the formation of the vortex once the fluid collides with the blades. However, it is possible to show that the standard rotor blades have a greater interaction with the fluid due to the number of blades. This interaction generates more drag force on the rotor therefore this becomes more torque generated.
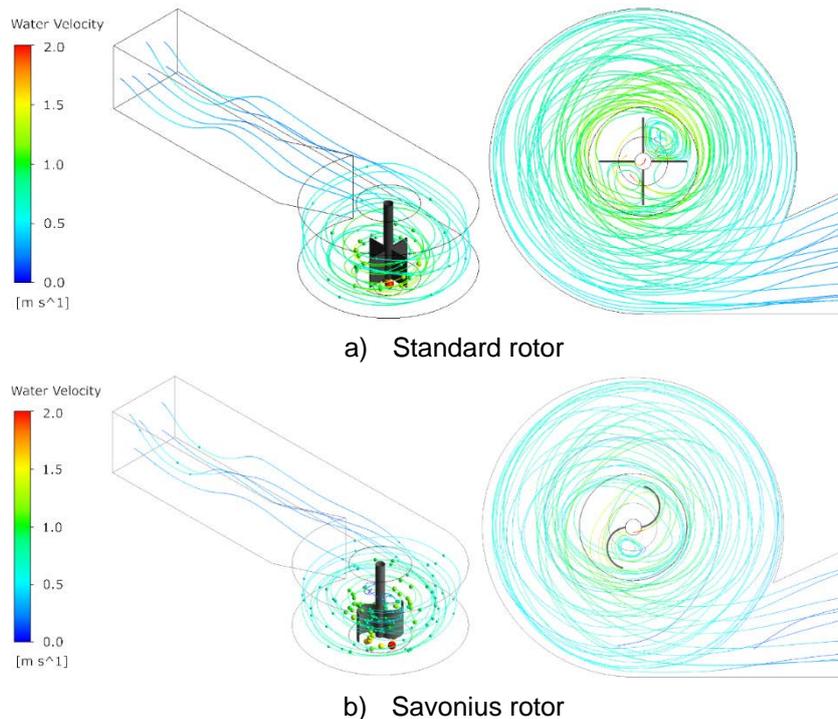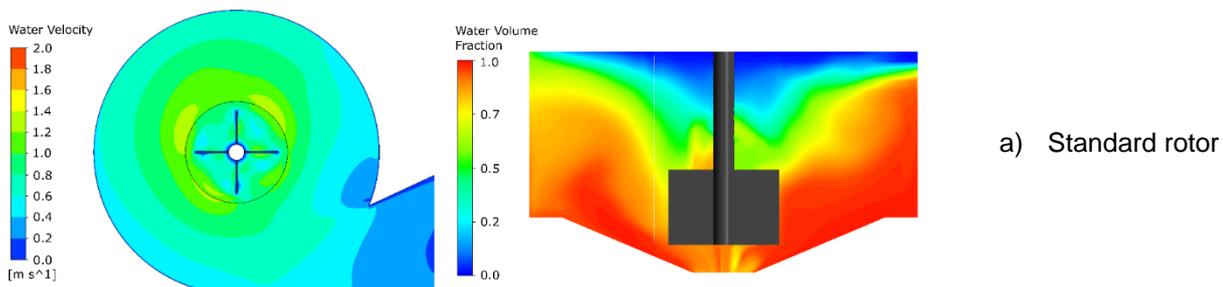

a) Standard rotor

b) Savonius rotor

Figure 8. Water streamlines for standard and Savonius rotor

To exemplify what was said above, Figure 9 represents the interaction between the fluid and the rotor. Two planes are shown, one horizontal and one vertical to represent contours of fluid velocity and volume fraction respectively. In this figure it can be seen how the vortex is distorted when it interacts with the rotor (volume fraction) and how the fluid drops its velocity when it also interacts with it (fluid velocity) reaching zero when it is close to the rotor blade.

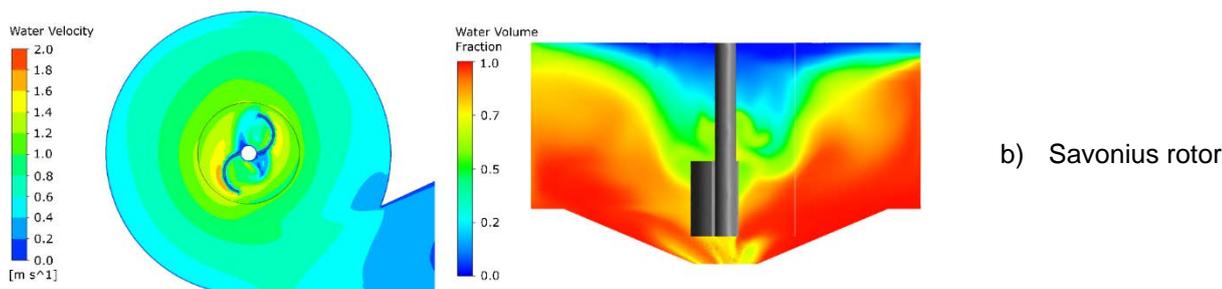a) Standard rotor

b) Savonius rotor

Figure 9. Water velocity and volume fraction

The difference between the Savonius rotor and the standard rotor lies in the number of blades. [25] shows that the efficiency of a Savonius rotor decreases with the increase of blades due to the negative torque (when the blade is moving backwards) that it presents. However, for this study, the fluid always rotates in the same direction and the rotor presented a negligible negative torque, since it is generated by the collision between the initial blade with the fluid and this changes the speed direction.

Contrary to what was said above, the Savonius rotor blades are the ones that present a smaller difference (18%) in their torque generation as the rpm increases with respect to the straight blades (20%). With this one could not speak of a significant difference between the two rotors, however, the number of blades in the Savonius rotor affected its performance.

5 CONCLUSION

The gravitational vortex turbine is projected as an alternative to pico-hydroelectric power plants. In recent years, there has been an increase in interest in these plants and several companies have dedicated themselves to building them, either for communities or companies that have a nearby water resource.

The Savonius rotor did not present the best performance. However, it had acceptable performance, even when the previous studies recommendations of using three blades instead of four were followed. On the other hand, this rotor improves its performance when there is greater drag force, and the negative torque does not generate losses in it.

It was shown that rotor design affects the performance of Gravitational Vortex Turbine. Given this, GVT studies should also focus on the design of the rotor (combined with tank design), since most of these studies have been carried out around the formation of the vortex in the chamber, which seek to increase the outlet velocity. This study is expected to mark a starting point to motivate the study on the gravitational vortex turbine and especially on the rotor design.

6 REFERENCES

[1] F. Zotlöterer, "Gravitational Water Vortex Power Plants," 2003. http://www.zotloeterer.com/welcome/gravitation-water-vortex-power-plants/configuration-function/ (accessed Mar. 04, 2018).

[2] H. feng LI, H. xun CHEN, Z. MA, and Y. ZHOU, "Formation and Influencing Factors of Free Surface Vortex in a Barrel with a Central Orifice at Bottom," *Journal of Hydrodynamics*, pp. 238–244, 2009, doi: 10.1016/S1001-6058(08)60141-9.

[3] J. Sierra, A. Ruiz, A. Guevara, and A. Posada, "Review: gravitational vortex turbines as a renewable energy," *International Journal of Fluid Machinery and Systems*, vol. 13, no. 4, 2020, doi: 10.5293/IJFMS.20xx.x.x.xxx.

[4] H. M. Shabara, O. B. Yaakob, Y. M. Ahmed, A. H. Elbatran, and M. S. M. Faddir, "CFD validation for efficient gravitational vortex pool system," *J Teknol*, vol. 74, pp. 97–100, 2015, doi: 10.11113/jt.v74.4648.

[5] Y. Nishi, R. Suzuo, D. Sukemori, and T. Inagaki, "Loss analysis of gravitation vortex type water turbine and influence of flow rate on the turbine's performance," *Renew Energy*, vol. 155, pp. 1103–1117, Aug. 2020, doi: 10.1016/J.RENENE.2020.03.186.

[6] M. H. Basri and A. Nasuki, "Water Discharge Management Based on Open and Closed Cylinders in the Gravitation Water Vortex Power Plant," *JEEE-U (Journal of Electrical and Electronic Engineering-UMSIDA)*, vol. 5, no. 1, pp. 22–36, Mar. 2021, doi: 10.21070/jeeeu.v5i1.1008.

[7] A. Ruiz Sánchez, J. Andrés, S. del Rio, and T. Pujol, "Numerical study and theoretical comparison of outlet hole geometry for a Gravitational Vortex Turbine," *Hal xx-xx Indonesian Journal of Science & Technology*, vol. 4, no. 1, pp. xx–xx, 2019, doi: 10.17509/ijost.v4i1.xxxx.

[8] S. Mulligan, J. Casserly, and R. Sherlock, *Experimental and numerical modelling of Free-Surface Turbulent Flows in Full Air-Core Water Vortices*, vol. 1. Nice: Onziémes Journées de L'Hydraulique, 2014. doi: 10.1007/978-981-287-615-7_37.

[9] S. Dhakal *et al.*, "Comparison of cylindrical and conical basins with optimum position of runner: Gravitational water vortex power plant," *Renewable and Sustainable Energy Reviews*, no. 48, pp. 662–669, 2015, doi: 10.1016/j.rser.2015.04.030.

[10] A. S. Saleem *et al.*, "Parametric study of single-stage gravitational water vortex turbine with cylindrical basin," *Energy*, vol. 200, p. 117464, Jun. 2020 doi: 10.1016/J.ENERGY.2020.117464.

[11] A. Ruiz Sánchez, J. A. Sierra-del Rio, A. J. Guevara Muñoz, and J. A. Posada-Montoya, "Numerical and Experimental Evaluation of Concave and Convex Designs for Gravitational Water Vortex Turbine," *Journal of Advanced Research in Fluid Mechanics and Thermal Sciences*, vol. 64, no. 1, pp. 160–172, 2019, doi: 2289-7879.

[12] S. R. Sreerag, C. K. Raveendran, and B. S. Jinshah, "Effect of outlet diameter on the performance of gravitational vortex turbine with conical basin," *Int J Sci Eng Res*, vol. 7, no. 4, 2016.

[13] S. Joshi and A. K. Jha, "Computational and Experimental Study of the Effect of Solidity and Aspect Ratio of a Helical Turbine for Energy Generation in a Model Gravitational Water Vortex Power Plant," *Journal of Advanced College of Engineering and Management*, vol. 6, pp. 213–219, Jul. 2021, doi: 10.3126/JACEM.V6I0.38360.

[14] T. C. Kueh, S. L. Beh, D. Rilling, and Y. Ooi, "Numerical Analysis of Water Vortex Formation for the Water Vortex Power Plant," *International Journal of Innovation, Management and Technology*, vol. 5, no. 2, pp. 111–115, 2014, doi: http://dx.doi.org/10.7763/IJIMT.2014.V5.496.

[15] L. Velásquez, A. Posada, and E. Chica, "Optimization of the basin and inlet channel of a gravitational water vortex hydraulic turbine using the response surface methodology," *Renew Energy*, vol. 187, pp. 508–521, Mar. 2022, doi: 10.1016/J.RENENE.2022.01.113.

[16] V. J. Alzamora Guzmán, J. A. Glasscock, and F. Whitehouse, "Design and construction of an off-grid gravitational vortex hydropower plant: A case study in rural Peru," *Sustainable Energy Technologies and Assessments*, vol. 35, pp. 131–138, Oct. 2019, doi: 10.1016/J.SETA.2019.06.004.

[17] A. Ruiz, A. Guevara, J. A. Sierra, and A. Posada, "Numerical comparison of two runners for gravitational vortex turbine," 2020.

[18] Wasserwirbel, "Genossenschaft Wasserwirbel Konzepte Schweiz," 2017. http://gwwk.ch/ (accessed Mar. 04, 2018).

[19] Green by Jonh;, "Vortex at Green School," 2015. http://greenbyjohn.com/vortex-at-green-school/ (accessed Apr. 10, 2018).

[20] Turbulent; "Turbulent micro hydropower," 2019. http://www.turbulent.be/ (accessed Mar. 04, 2018).

[21] KCT, "KOURIS CENTRI TURBINE," 2016. http://www.kcthydropower.com/

[22] Wasserwirbelkraftwerk, "Wasserwirbelkraftwerk," 2017. http://wasserwirbelkraftwerk-de.simplesite.com/434308050

[23] R. Dhakal *et al.*, "Technical and economic prospects for the site implementation of a gravitational water vortex power plant in Nepal," in *IEEE International Conference on Renewable Energy Research and Applications (ICRERA)*, 2016, pp. 1001–1006. doi: 10.1109/ICRERA.2016.7884485.

[24] A. Laaraba and A. Khechekhouche, "Numerical simulation of natural convection in the air gap of a vertical flat plat thermal solar collector with partitions attached to its glazing," *Indonesian Journal of Science and Technology*, vol. 3, no. 2, pp. 95–104, 2018, doi: 10.17509/ijost.v3i2.12753.

[25] A. Kumar and R. P. Saini, "Performance parameters of Savonius type hydrokinetic turbine – A Review," *Renewable and Sustainable Energy Reviews*, vol. 64, pp. 289–310, 2016, doi: 10.1016/j.rser.2016.06.005.

[26] Y. L. Castañeda Ceballos, M. Cardona Valencia, D. Hincapié Zuluaga, J. Sierra Del Rio, and S. Vélez García, "Influence of the Number of Blades in the Power Generated by a Michell Banki Turbine," *International Journal of Renewable Energy Research - IJRER*, vol. 7, no. 4, pp. 1989–1997, 2017, doi: https://doi.org/10.20508/ijrer.v7i4.6372.g7246.

[27] D. Beltran-Urango, J. L. Herrera-Díaz, J. A. Posada-Montoya, L. Castañeda, and J. A. Sierra-del Rio, "Generación de Energía Eléctrica Mediante Vórtices Gravitacionales," in *MEMORIAS EXPO TECNOLOGIAS 2016, Medellin, Antioquia*, 2016, pp. 90–107.

[28] Du, Jiyun, Shen, Zhicheng, Yang, and Hongxing, "Effects of different block designs on the performance of inline cross-flow turbines in urban water mains," *Appl Energy*, vol. 228, pp. 97–107, 2018, doi: 10.1016/j.apenergy.2018.06.079.

[29] Ansys Inc., "User Manual Ansys ICEM CFD 12.1," vol. 0844682, no. November, pp. 724–746, 2009.

[30] R. S. S. Mulligan, J. Casserly, "Experimental and numerical modelling of Free-Surface Turbulent Flows in Full Air-Core Water Vortices," *Advances in Hydroinformatics*, pp. 549–569, 2014.